Article

Elevation Gradients Limit the Antiphase Trend in Vegetation and Its Climate Response in Arid Central Asia

Yujie Yang [1], Wei Huang [1,*], Tingting Xie [1], Chenxi Li [1], Yajie Deng [1], Jie Chen [1,2], Yan Liu [1] and Shuai Ma [1]

1   Key Laboratory of Western China's Environmental Systems (Ministry of Education), College of Earth and Environmental Sciences, Lanzhou University, Lanzhou 730000, China
2   College of Atmospheric Sciences, Lanzhou University, Lanzhou 730000, China
*   Correspondence: whuang@lzu.edu.cn

Abstract: Vegetation in arid central Asia (ACA) has been experiencing significant changes due to substantial warming and humidification since the 1980s. These changes are inhomogeneous due to the ecological vulnerability and topographic complexity of ACA. However, the heterogeneity of vegetation changes has received limited attention in the literature, which has focused more on the region's overall general features. Thus, this paper analyzes the regional heterogeneity of vegetation changes during the growing season in ACA and further explores their underlying drivers. The results reveal an antiphase trend of vegetation, with an increase in eastern ACA and a decrease in western ACA. This antiphase pattern is primarily constrained by the divergent hydrothermal and climatic contexts of different elevation gradients. At elevations higher than 300 m (in the eastern ACA), increased growing season precipitation dominates vegetation greening. Conversely, vegetation at elevations lower than 300 m (in western ACA) is influenced by growing season soil water, which is driven by winter precipitation (pre-growing season precipitation). Additionally, the temperature could indirectly impact vegetation trends by altering precipitation, soil water, glaciers, snow cover, and runoff. Our findings have implications for restoring the ecosystem and sustainable development in ACA.

Keywords: vegetation; antiphase trend; elevational gradients; direct effect; lag effect

1. Introduction

Climate change alters hydrological cycle processes such as snow cover, runoff, and soil water, which affect the ecosystem [1]. As the most critical component of the ecosystem, vegetation activities could well represent ecosystem variations [2], and vegetation is highly sensitive to climate change [3–5], especially in arid ecosystems [6]. For example, dryland vegetation was observed as having a robust increase in precipitation sensitivity [7]. Increased precipitation provides favorable conditions for vegetation growth [1,8] and vice versa [6]. Warming potentially limits vegetation growth by reducing water resource availability [1] and affecting vegetation productivity [9,10]. The dynamics of soil water also significantly affect vegetation. For instance, increased global vegetation greenness has begun to level off due to growing soil moisture limitations [11]. Additionally, a lack of soil water even results in a regional or worldwide decline in the greenness of vegetation [12,13]. In addition, glaciers, snow cover [14], and permafrost [15,16], as essential parts of eco-hydrological processes, also contribute to vegetation change. Arid central Asia (ACA, including arid central Asia and Xinjiang in China) is controlled by the mid-latitude westerly circulation, its distance from the ocean, making water vapor transport difficult to reach, and the perennial descending motion in the lower and middle troposphere, making it the world's largest non-zonal arid zone [17]. ACA is characterized by fast warming, scarce precipitation, and ecosystem vulnerability [17–22]. A series of studies have focused on ACA vegetation and its driving factors in recent decades [1,5,23,24]. For example, Zhao et al.

pointed out that most numbers of pixels related to vegetation in central Asia increased in the growing season and spring from 1982 to 2003, which is highly correlated with current precipitation and evapotranspiration [5]. Some researchers showed a transition of vegetation change from increasing to degrading in the 1990s in central Asia, and water deficits explain a large part of this transition [1,23,24]. Meanwhile, vegetation in Xinjiang has been increasing significantly since the 1980s [25,26].

Previous research has concentrated more on the isolated features of vegetation changes in central Asia and Xinjiang, or the overall changes in ACA. However, ACA has a complex topography, with elevation ranging from -156 to 8238 m, which results in divergent vegetation change and the region's response to the climate at different elevation gradients [27,28]. Although there is a vertical lapse rate associated with temperature, it is not the sole dominant factor causing the divergent changes [28]. Furthermore, the eastern part of ACA (Xinjiang in northwest China) has been experiencing climatic warming and humidification in recent decades [29–31], whereas central Asia shows a drying trend [32]. The difference in the climate change in ACA may exacerbate the existing divergent vegetation changes at varying elevations. However, the heterogeneity in vegetation changes at different elevation gradients and the related climate effects are still unknown in ACA. Thus, we aim to understand the impact of elevation on heterogeneity in vegetation changes in ACA.

In this study, we first investigated the spatiotemporal variations of vegetation from 1982 to 2015 in ACA using a normalized differential vegetation index (NDVI) dataset over two elevation gradients and vegetation types. Meanwhile, the independent and interactive effects of natural factors on vegetation were investigated using the linear mixed effect model (LMM). Furthermore, the direct and indirect effects were separated by the structural equation model (SEM). These explorations can provide constructive suggestions for the efficient use of water resources and the ecologically sustainable development of the region.

2. Materials and Methods

2.1. Overview of the Study Area

The study area is the core region of arid central Asia, ranging in latitude from 36°N to 50°N and longitude from 50°E to 90°E. According to the aridity index [33], the region covers arid, semi-arid, and dry sub-humid areas (Figure 1a). The area covers 5.18 million km^2, and the desert covers nearly 40%. ACA warms rapidly, reaching 1.6 °C over the century [34], with winter precipitation dominating in the west and summer precipitation in the east (Figure 1b,c) [35]. The topography of ACA is complex, with elevation differences higher than 7000 m. The low elevations have high temperature and low precipitation with annual precipitation less than 300 mm; at high elevations such as the Tianshan Mountains, precipitation is relatively high, and glacial melt has gradually increased in recent years due to climate warming, which causes runoff to increase [14,31].

2.2. Data

2.2.1. Vegetation Index

NDVI is an important indicator of vegetation activity, even in mountainous areas [7,35,36]. The Global Inventory Modelling and Mapping Studies (GIMMS) NDVI 3g v1 dataset was used in this study. This dataset is derived from the advanced very high-resolution radiometer (AVHRR). The 8 km resolution GIMMS NDVI 3g v1 dataset has a temporal resolution of 16 days and covers the period of 1982–2015 [37]. We combined the original data into the monthly, growing season, and yearly scales using the maximum value composite (MVC). The MVC can effectively reduce the effect of clouds, atmosphere, solar altitude, etc. [38].
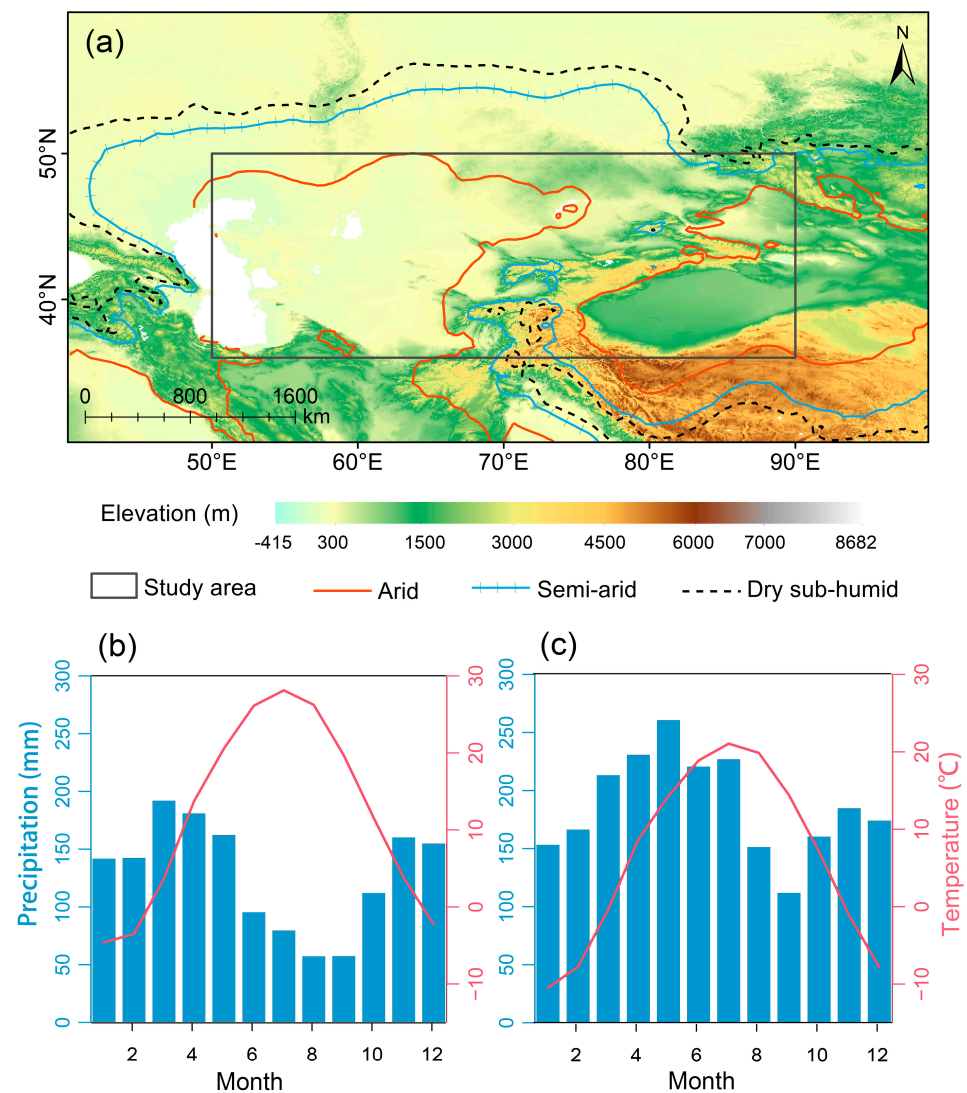
Figure 1. (**a**): Location and topographic characteristics of the study area. The rectangle with a black border is the study area of this study. The different shapes and colors of lines are the dividing lines between arid, semi-arid, and dry sub-humid areas. The average monthly temperature and precipitation in the western arid central Asia (ACA) (**b**) and the eastern ACA (**c**). The blue bars represent precipitation, and the red curves represent temperature.

2.2.2. Datasets of Effect Factors

The monthly precipitation data were obtained from the Global Precipitation Climatology Centre (GPCC, http://gpcc.dwd.de/, accessed on 22 November 2022) at Deutscher Wetterdienst (DWD). We used the GPCC Full Data Monthly Product dataset with a resolution of $0.25° \times 0.25°$, which is the most accurate in situ precipitation reanalysis dataset in the GPCC [39].

The monthly temperature data with a resolution of $0.5° \times 0.5°$ was provided by UK's National Centre for Atmospheric Science (NCAS) at the University of East Anglia's Climatic Research Unit (CRU), which is one of the most widely used climate datasets (https://crudata.uea.ac.uk/cru/data/hrg/, accessed on 22 November 2022) [40]. We selected version CRU TS4.05 for our analysis.

The European Center for Medium-Range Weather Forecasts' Reanalysis (ECMWF) provides a consistent view of the evolution of land variables from 1981 to present (https://www.ecmwf.int/, accessed on 22 November 2022) [41]. The soil water and snow cover data in this dataset have been proven to be applicable and the soil water is divided into four layers (0–7 cm,

7–28 cm, 28–100 cm, and 100–289 cm). We chose the surface layer (0–7 cm) and the second layer (7–28 cm) to represent the soil water conditions in the study area [42].

2.2.3. Vegetation Types and DEM

Vegetation types were obtained from the European Space Agency (ESA) Climate Change Initiative (CCI), where a time series of consistent global LC maps at 300 m spatial resolution on an annual from 1992 to 2015 is available (http://maps.elie.ucl.ac.be/CCI/viewer/download.php, accessed on 22 November 2022). According to the International Geosphere-Biosphere Programme (IGBP) and related research [41], ESA CCI LC is categorized into six vegetation types in this study: forests, open vegetation, grasslands, croplands, shrubs, and bare land.

The digital elevation model (DEM) data is provided by NASA's Shuttle Radar Topography Mission (SRTM), which is available for download from https://www.usgs.gov/centers/eros, accessed on 22 November 2022.

2.3. Methods
2.3.1. Trends and Regression Analysis

The Theil–Sen median trend analysis and Mann–Kendall test were used to evaluate trends in growing season average NDVI from 1982 to 2015 [43–45], as they are robust nonparametric statistical methods for trend detection. We used the function "*trend_manken*" provided by NCAR Command language (NCL) version 6.6.2 [46] (https://www.ncl.ucar.edu/, accessed on 22 November 2022) to conduct the trend analysis and test it. Moreover, the regions where $p \leq 0.05$ were considered statistically significant in this study. The temporal trends of growing season factors and of vegetation response to these factors were performed by linear regression analysis and correlation analysis using the functions "*regCoef*" and "*escorc_n*" in NCL.

2.3.2. Linear Mixed-Effect Model (LMM)

The linear mixed-effect model (LMM) is widely used because it: (1) enables the simultaneous estimation of the effects of multiple variables and their interactions on the dependent variable; (2) takes into account random effects from different repeated measurements; and (3) quantifies the degree to which those factors explain vegetation change [47–50]. In this study, the LMM was used to assess the effects of temperature, precipitation, snow cover, and soil water on vegetation. The LMM analysis was carried out in R language [51] using the "*lme4*" package [52], and *p* values for fixed-effect parameters were estimated using the "*lmerTest*" package [53]. The optimal model was selected according to the reasonableness of the assumptions, coefficient of determination (R^2), and the smaller AIC (Akaike information criterion) [54]. Finally, we constructed the best-fit model by considering the four factors and their interactions as fixed effects and treating vegetation types and elevation gradients as random variables.

2.3.3. Structural Equation Model (SEM)

The structural equation model (SEM) separates the proposed direct and indirect components and their interactions. SEM also enables us to quantify the relative relevance of each factor via the path coefficients (PC) [9,15,47]. SEM analysis was carried out using AMOS software version 24.0 [55,56] and the "*lavaan*" package in R [57], and the results were consistent between the two programs. AMOS results are reported in this study as it generates both unstandardized and standardized outputs. The PCs and parameters are estimated using the maximum likelihood method. Here, we propose three hypotheses: (1) The vegetation is directly impacted by temperature, precipitation, snow cover, and soil water. (2) Snow cover and precipitation indirectly affect vegetation through soil water. (3) Temperature indirectly affects vegetation through precipitation, snow cover, and soil water.

3. Results

3.1. Characteristics of Vegetation Variations in ACA

Vegetation in ACA grows primarily from May to September in the east and from April to October in the west (Figure 2b) [58]. These time periods are defined as the growing season of the eastern and western ACA, respectively. The temporal variation of growing season NDVI in ACA has been greening at 0.0002 yr^{-1} since 1982 (Figure 3b). However, the changes in NDVI are characterized spatially by antiphase patterns (Figure 2a). The greening (0.0005 yr^{-1}) area is mainly in eastern ACA, accounting for 43.21% of the study area (Figures 2c and 3b). The browning (−0.0004 yr^{-1}) area is mainly in western ACA, accounting for 56.79% (Figures 2c and 3b). By counting the trends of NDVI at different elevation gradients, this boundary coincides more with a 300 m elevation (the solid black line in Figure 2a and the gray shade in Figure 3a). In summary, the vegetation of most grids in ACA shows a decrease at elevations lower than 300 m and an increase at elevations higher than 300 m, which has also been proven in other growing season scales and an annual scale (figure omitted).
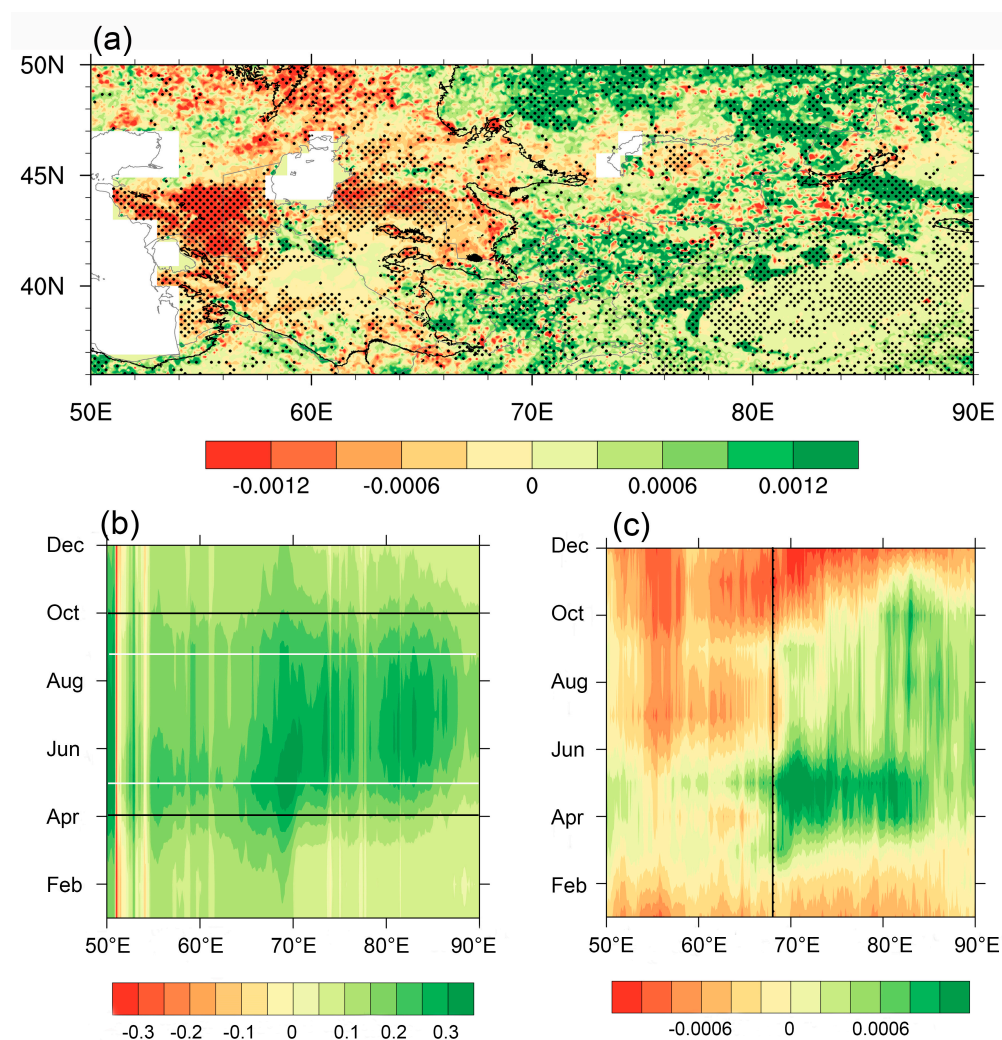

Figure 2. (**a**): Spatial distribution of growing season NDVI trends in ACA from 1982 to 2015. The solid black curve is the boundary at an elevation of 300 m, its west side is the area with an elevation lower than 300 m and the east side is the area with an elevation higher than 300 m. The black dots are areas that passed the significance test ($p < 0.05$); (**b**): cross-sectional plots of monthly distributions of the average value of NDVI, with the white lines showing May and September and the black lines showing April and October; (**c**): cross-sections of monthly vegetation trends, with the black line in the range of 65°E to 70°E.
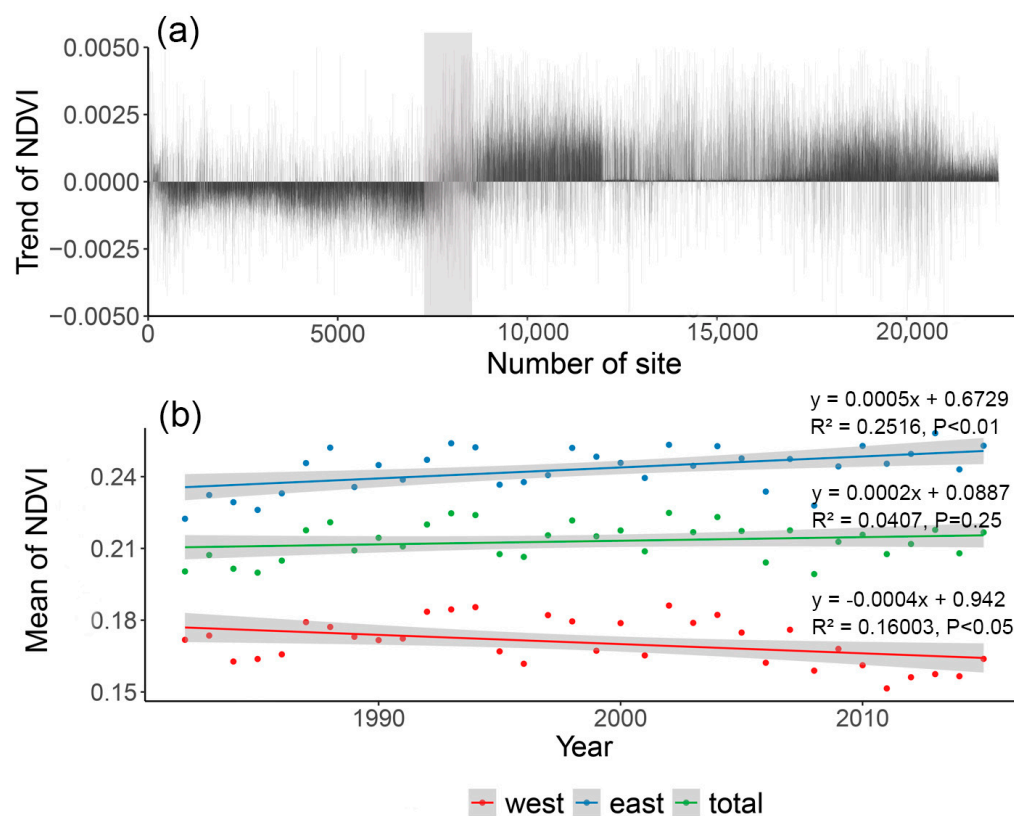
Figure 3. (**a**): NDVI trends during the growing season at different elevations. The X-axis represents all grid points in ACA arranged by elevation instead of the actual elevation as multiple grid points share one elevation; the gray shaded band represents the area where elevation is around 300 m; (**b**): changes in the mean values of growing season NDVI. Green represents the whole region of ACA; red represents the western region of ACA (elevation lower than 300 m), and blue represents the eastern region of ACA (elevation higher than 300 m).

3.2. Response of Vegetation to Factors

Previous studies have demonstrated the influence of anthropogenic and natural climatic factors on vegetation formation, classification, and change [45,59–62]. In the water-scarce and arid ACA regions, the response of vegetation to climatic factors [1] (e.g., temperature, precipitation), and especially natural factors related to water resources [24,31] (e.g., soil water and snow cover), has attracted our attention. In Figure 4, we can see that trends of these elements show an antiphase distribution in ACA bounded by 300 m. Specifically, in the western ACA, there was a significant and dramatic increase in temperature (Figure 4a), as well as widespread decreases in precipitation (Figure 4c) and soil water (Figure 4e), and the snow cover is absent (Figure 4g). In eastern ACA, there was a moderate increase in temperature (Figure 4a) and an increase in precipitation (Figure 4c) and soil water (Figure 4e). At the same time, snow cover was significantly reduced (Figure 4g). Regression analysis further demonstrates that there is also a different distribution of regression coefficients among temperature, snow cover, and NDVI in eastern and western ACA (Figure 4b,h). Nevertheless, there is a broad and significant positive correlation between precipitation, soil water, and NDVI in the overall area (Figure 4d,f).

These results demonstrate that the differences in climate context and hydrothermal conditions between the eastern and western of ACA affect NDVI. However, it remains difficulty of explaining the antiphase changes of NDVI using any individual elements. We, therefore, hypothesize that all these factors interact and that these interactions may affect vegetation, and we verify this hypothesis in the following subsections.
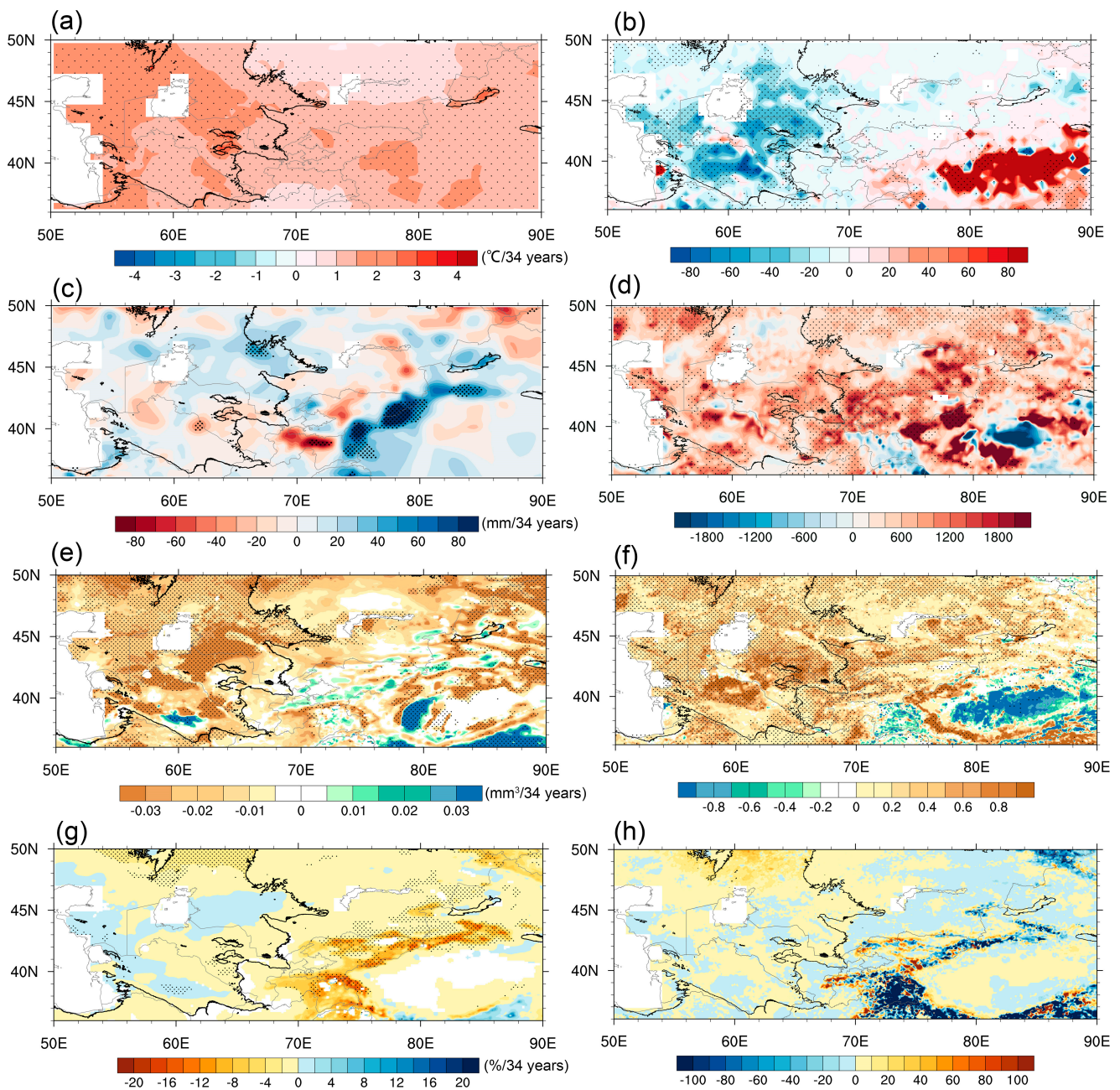
Figure 4. Distribution of trends in temperature (**a**), precipitation (**c**), soil water (**e**), and snow cover (**g**). Distribution of regression coefficients between temperature (**b**), precipitation (**d**), soil water (**f**), and snow cover (**h**) with NDVI. The black dots are areas that passed the significance test ($p < 0.05$).

3.3. Liner Mixed Effect of Factors on NDVI

The LMM was utilized in this study to distinguish the independent and interactive effects of temperature, precipitation, soil water, and snow cover on NDVI. In the LMM, the following variables were set as fixed effects: temperature, precipitation, snow cover, soil water, and their interactions; vegetation types and elevation gradients were set as random effects. The results show that soil water, snow cover and precipitation and have the greatest effect on NDVI, with estimates of 4.37×10^{-1}, 2.66×10^{-1}, 2.44×10^{-1} ($R^2 = 0.80$, $p < 0.001$), respectively, which is consistent with the previous regression analysis. The interactions between temperature and precipitation ($p < 0.001$), temperature and snow cover ($p < 0.001$), precipitation and soil water ($p < 0.001$), and snow cover and soil water ($p < 0.001$) all have significant effects on NDVI (Table 1).

Table 1. Results of linear mixed-effects models of temperature (Tmp), precipitation (Pre), snow cover (Snow C), soil water (Soil W), and their interaction on NDVI.

		Estimate	**p Value**
Fixed Effect	(Intercept)	-4.28×10^{-2}	8.61×10^{-1}
	Tmp	-7.84×10^{-3}	3.44×10^{-1}
	Pre	2.44×10^{-1}	$<2 \times 10^{-16}$ ***
	Soil W	4.37×10^{-1}	$<2 \times 10^{-16}$ ***
	Snow C	2.66×10^{-1}	$<2 \times 10^{-16}$ ***
	Tmp: Pre	2.77×10^{-2}	1.18×10^{-7} ***
	Pre: Soil W	6.03×10^{-2}	$<2 \times 10^{-16}$ ***
	Tmp: Soil W	1.83×10^{-2}	3.07×10^{-3} **
	Temp: Soil C	1.31×10^{-1}	$<2 \times 10^{-16}$ ***
	Soil W: Snow C	-1.32×10^{-1}	$<2 \times 10^{-16}$ ***
	Groups Name	**Variance**	**Std.Dev.**
Random Effect	Elevation gradients	0.25	0.50
	Vegetation types	0.18	0.43
	Residual	0.24	0.50

Significant codes: 0 '***' 0.001 '**' .

Random effects on elevation gradients and vegetation types are also observed, with a variance of 0.25 and 0.18, accounting for 37.01% and 17.89% of the total residuals, respectively (Table 1). This means that they can explain almost 50% of the residual, indicating that the effect of factors on vegetation is indeed divergent in different vegetation types and elevational gradients.

3.4. SEM Results of Two Elevational Gradients

The antiphase trends in vegetation over the elevation gradients are proven in Section 3.1. Meanwhile, hypotheses of independent and interactive effects of factors on vegetation simultaneously are presented in Section 3.2. The above results are then proven by using LMM in Section 3.3. Here, SEM was conducted to further investigate how these interactions affect vegetation directly and indirectly. The results reveal that at elevations lower than 300 m, all hypothesized paths can account for 58% of the total variation in NDVI ($R^2 = 0.58$). For direct effect, soil water contributes the most to NDVI, with the PC being 0.64, followed by precipitation, snow cover, and temperature, with PCs of 0.17, 0.15, and 0.09, respectively. In terms of the total effect, soil water is still the most impacted factor (PC = 0.64). The total effect of precipitation on NDVI (PC = 0.35) is greater than the direct effect (PC = 0.17) because it has an indirect effect (PC = 0.28) through soil water. Although the temperature has a direct positive effect on NDVI, the total effect is negative (PC = −0.44) because temperature affects NDVI through precipitation (PC = −0.59), snow cover (PC = −0.56), and soil water (PC = −0.24) as a negative indirect effect, which outweighs the direct effect (PC = 0.09) (Figure 5a and Table 2). In summary, at elevations lower than 300 m, high temperatures accompanied by little precipitation led to a decrease in soil water, which may also be related to increase in evaporation due to warming. This is the reason for vegetation degradation at elevations lower than 300 m.
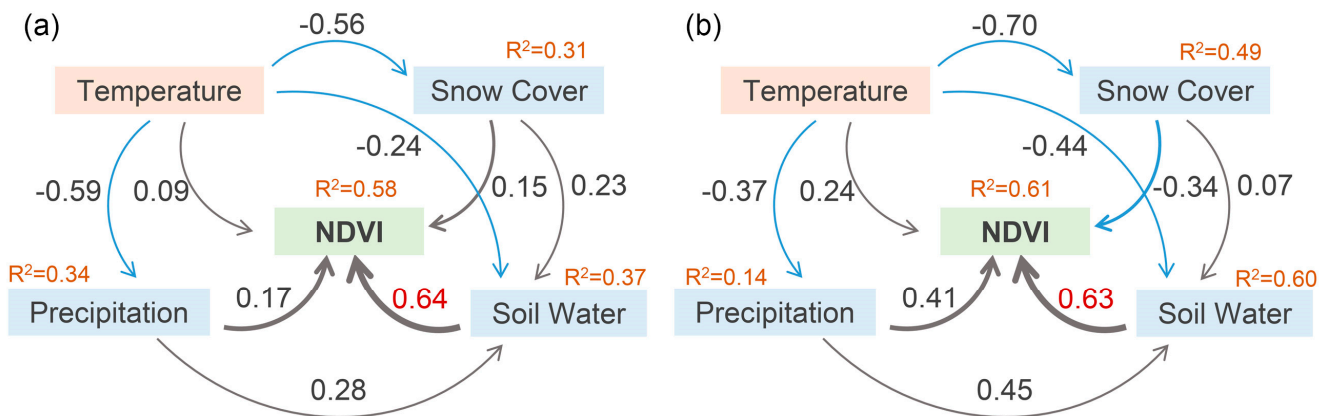
Figure 5. Direct and indirect effects of temperature, snow cover, precipitation, and soil water on NDVI in areas lower than 300 m (**a**) and higher than 300 m (**b**). Gray arrows represent positive correlations, blue arrows represent negative correlations, and thicker arrows represent larger PCs.

Table 2. The total, direct and indirect effects of temperature (Tmp), precipitation (Pre), snow cover (Snow C), and soil water (Soil W) on NDVI at different elevation gradients and time scales.

		Growing Season (Elevation < 300 m: Apr~Oct, Elevation > 300 m: May~Sep)			Year			Growing Season NDVI with Tmp, Snow C, Soil W, and Winter Pre		
		Total	Direct	Indirect	Total	Direct	Indirect	Total	Direct	Indirect
Elevation <300 m	Tmp	−0.44	0.09	−0.52	−0.37	0.23	−0.59	−0.44	−0.10	−0.33
	Pre	0.35	0.17	0.18	0.49	0.36	0.13	0.41	0.22	0.19
	Snow C	0.30	0.15	0.15	0.44	0.31	0.13	0.30	0.16	0.14
	Soil W	0.64	0.64	0.00	0.45	0.45	0.00	0.58	0.58	0.00
Elevation >300 m	Tmp	−0.08	0.24	−0.32	0.02	0.07	−0.06	−0.08	0.12	−0.20
	Pre	0.69	0.41	0.28	0.67	0.50	0.18	0.51	0.26	0.25
	Snow C	−0.30	−0.34	0.04	−0.18	−0.41	0.24	−0.42	−0.41	0.01
	Soil W	0.63	0.63	0.00	0.50	0.50	0.00	0.73	0.73	0.00

For elevations higher than 300 m, the hypothesized pathways explain 61% of the variation in the NDVI (R^2 = 0.61). Soil water still contributes the most in terms of direct effects (PC = 0.63), followed by precipitation (PC = 0.41), snow cover (PC = −0.34), and temperature (PC = 0.24). In terms of the total effect, the results are divergent. Precipitation is the most impacted factor (PC = 0.69), with an indirect effect on the NDVI (PC = 0.28) by affecting the soil water (PC = 0.45). The snow cover at high elevations negatively affects the NDVI as a PC of −0.34. The effect of temperature on the NDVI is more complex. The temperature has the smallest direct effect (PC = 0.24) on the NDVI but contributes the largest indirect effect (PC = −0.32) among the four factors. Temperature indirectly affects NDVI through precipitation (PC = −0.37), snow cover (PC = −0.70), and soil water (PC = −0.44). That is, warming leads to less snow cover, and the increased runoff from melting snow promote vegetation growth. Conversely, the warming-induced decrease in soil water is detrimental to vegetation growth (Figure 5b and Table 2).

In summary, vegetation in both western and eastern ACA are more sensitive to water resources (e.g., precipitation and soil water) than temperature. Soil water significantly impacts vegetation at elevations lower than 300 m in terms of the direct and total effects. At elevations higher than 300 m, soil water still has the greatest direct effect on vegetation, while precipitation has the greatest total effect. Furthermore, the direct effect of temperature on vegetation is positive, but the indirect effect is negative, resulting in a smaller total effect of temperature after the direct and indirect effects are canceled out.

3.5. Lagging Response of Growing Season Vegetation to Winter Precipitation

By comparing the total effects at the annual and growing season scales, we found that precipitation had a greater effect on NDVI than soil water at elevations lower than 300 m at annual scale (Table 2). The asymmetric results on the annual and growing season scales imply that last year's winter precipitation influences next year's growing season vegetation. Here, winter precipitation refers to the pre-growing season precipitation (December of the previous year to next April for eastern ACA, and December of the previous year to next March for western ACA). Previous studies have shown that the eastern ACA is dominated by summer precipitation, and the western ACA is dominated by winter precipitation (including areas lower than 300 m in this study) [63,64]. Meanwhile, as shown in Figure 5, precipitation indirectly affects vegetation via soil water. Therefore, the connection between winter precipitation and growing season vegetation in the western ACA cannot be neglected.

First, there is a significant correlation between the winter precipitation to growing season NDVI (Figure 6a) and soil water (Figure 6b) in western ACA. In addition, we conducted SEM analyses of winter precipitation with the growing season NDVI, and the results are reported in Table 2 (replacing growing season precipitation with winter precipitation only, leaving other growing season factors unchanged). The results show that winter precipitation has a greater effect (PC = 0.41) on the growing season NDVI than growing season precipitation (PC = 0.35) at elevations lower than 300 m. Meanwhile, the total effect of soil water on the growing season NDVI (PC = 0.73) also increased significantly compared to the annual scale (PC = 0.50), which was caused by winter precipitation.

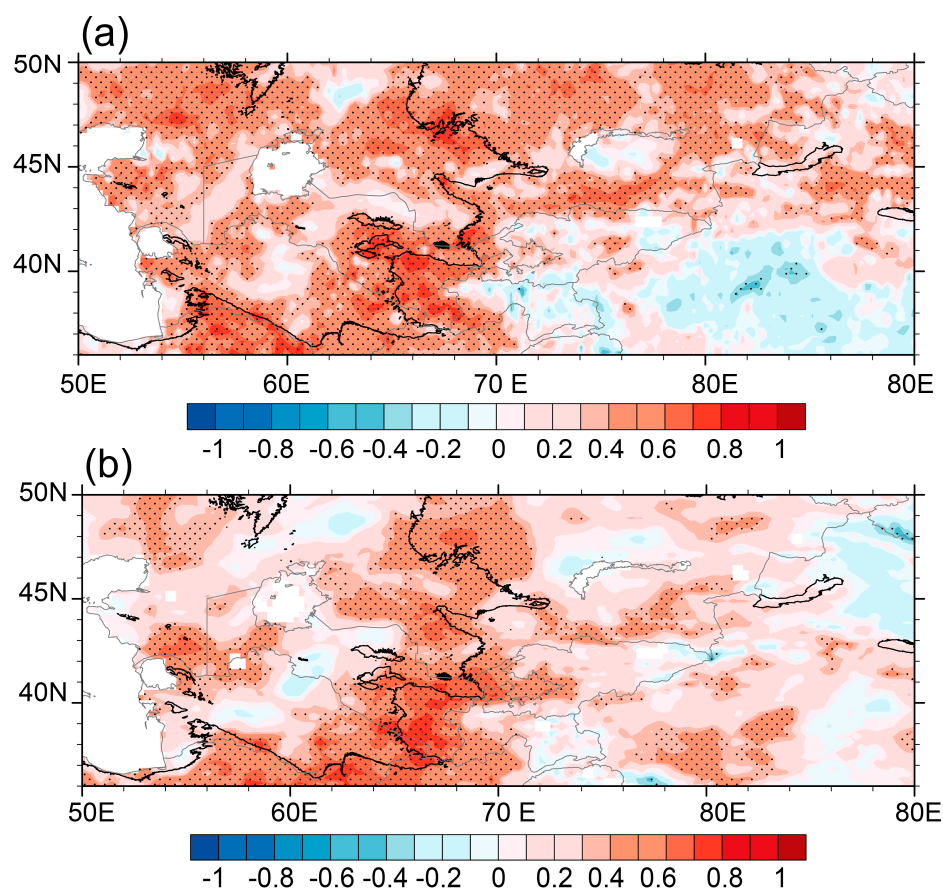**Figure 6.** (**a**): The lagged response of NDVI to precipitation. Distribution of correlation coefficients between winter precipitation (here referring to the pre-growing precipitation) and growing season NDVI; (**b**): distribution of correlation coefficients between winter precipitation and growing season soil water.

These findings support the hypothesis at the beginning of this subsection, which states that vegetation is more vulnerable to winter precipitation at elevations lower than 300 m than growing season precipitation. Growing season vegetation has a lag response on winter precipitation [5], and winter precipitation affects growing season vegetation via the growing season soil water.

4. Discussion

Our study identifies an elevation divergence in growing season vegetation trends in ACA, which is also observed in the figures of Burrell et al.'s study [65]. This study by Burrell et al. takes a global outlook without focusing on ACA or identifying and isolating the specific climate elements that affect the region. We further discovered that precipitation has the greatest total effect on vegetation greening at higher elevations, while soil water has the greatest effect on browning at lower elevations. These findings provide the basis for a further understanding of the vegetation in ACA. Nevertheless, the characteristics of the divergence in different vegetation types, as well as other factors affecting vegetation at different altitude gradations, still need to be discussed.

4.1. SEM Results of Different Vegetation Types

Table 1 shows that vegetation types explain a large percentage of residuals in addition to elevation gradients. Therefore, in this section, we discuss the direct and indirect factors of the NDVI according to the different vegetation types. In particular, we discuss the effect of soil water at different layers on vegetation.

On the one hand, the effects of the four factors on vegetation are different for various vegetation types. Bare land is the predominant kind of land cover in areas lower than 300 m, followed by open vegetation, waterbodies, shrubs, grasslands, cropland, and forests (Figure 7a). Even though bare land is often considered devoid of vegetation, we nevertheless consider it since some discontinuous and sparse vegetation exists that was previously neglected [60,66]. The results of SEM analysis exhibit that the NDVI on bare land is mainly dominated by soil water in terms of total effect and direct effect (PC = 0.66) (Figure 7c), which is the same conclusion as in Section 3.4. In areas higher than 300 m, grasslands dominate the area (Figure 7a). Since precipitation is the most important impact factor for grasslands (Figure 7d), the result also proves that precipitation strongly affects vegetation in the high elevation gradient.
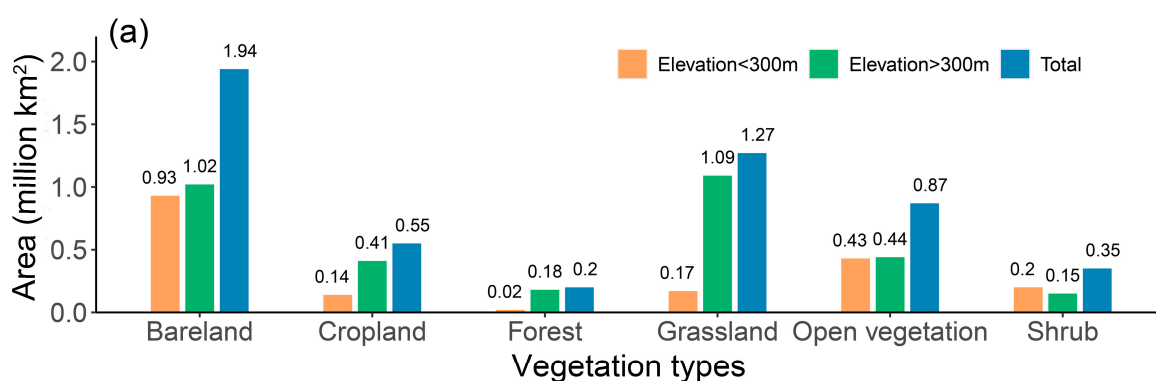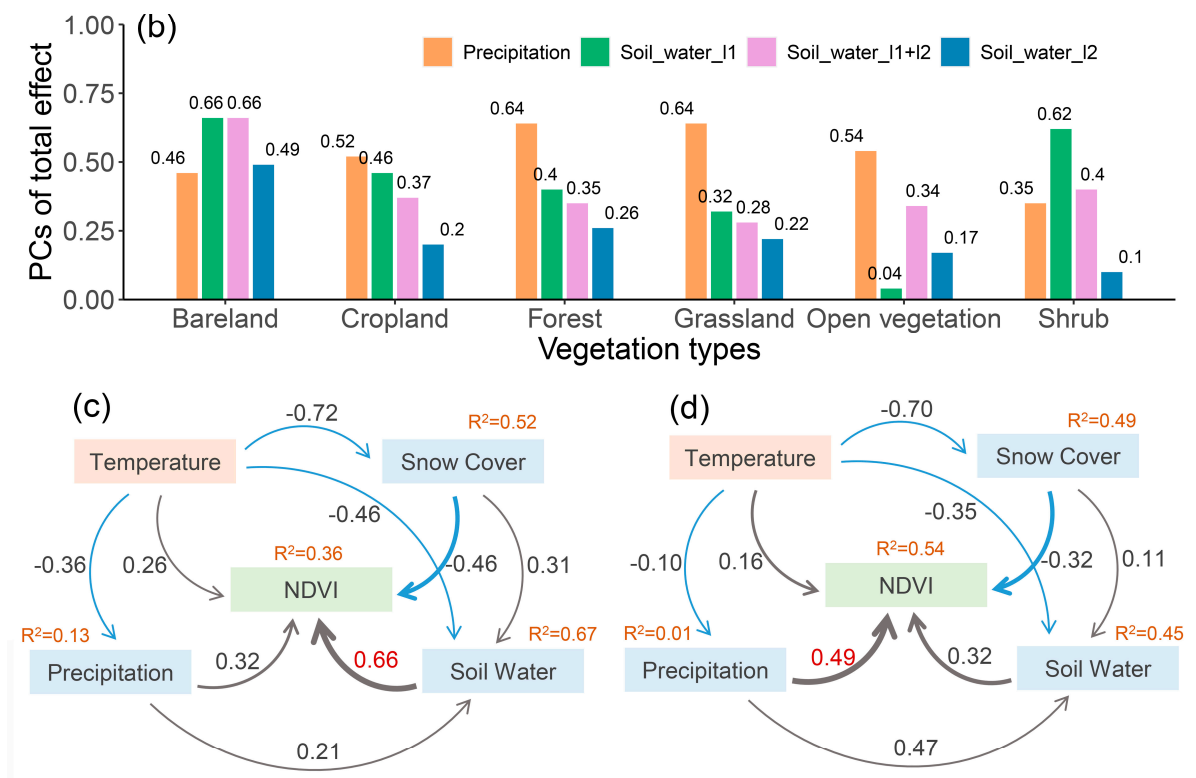
Figure 7. *Cont.*

Figure 7. Area of different vegetation types at different elevation gradients: (**a**) total effects of precipitation, the first layer of soil water, the second layer of soil water, and the total of the two layers of soil water on vegetation. (**b**) The "soil_water_l1" is the first layer of soil water, "soil_water_l2" is the second layer of soil water, and "soil_water_l1+l2" is the sum of the two layers. SEM results for bare land (**c**) and grassland (**d**). Gray arrows represent positive correlations, blue arrows represent negative correlations, and thicker arrows represent larger PC.

On the other hand, soil water at different levels, especially near the surface, affects the vegetation because the depth of the root is different for various vegetation types. By comparing the total effects of precipitation, the first layer of soil water, the second layer of soil water, and the total of the two layers of soil water on vegetation (Figure 7b), we found that the total effect of soil water in the second layer was more significant in bare land. This is because, in arid bare land, sparse vegetation needs to root deep underground to find the water to sustain it.

4.2. Other Effects on Vegetation in the Low-Elevation Gradient

Precipitation is considered the main limiting factor for vegetation in arid zones in most previous studies [67,68]. However, our study shows that soil water is the dominant factor at low altitudes in ACA. Nevertheless, these findings do not contradict the previously mentioned before because both growing season precipitation (PC = 0.28) and winter precipitation (PC = 0.33) significantly directly affect growing season soil water at elevations lower than 300 m (Table 3, Figure 6). Meanwhile, Moore et al. also proved that the restoration of soil water deficits during the summer dry season occurs with a time lag from the winter precipitation of last year [69], which explains the decrease in soil water in this area. Additionally, the temperature has a large negative total effect on soil water (Table 3), so a large increase in temperature in western ACA (Figure 4a) will reduce soil water and thus affect vegetation growth.

Table 3. The total, direct and indirect effects of temperature (Tmp), precipitation (Pre), Winter precipitation (Winter Pre), and snow cover (Snow C) on soil water (Soil W) at elevations lower than 300 m.

	Total Effect	Direct Effect	Indirect Effect
Tmp	−0.53	−0.24	−0.29
Pre	0.28	0.28	0
Winnter Pre	0.33	0.33	0
Snow C	0.23	0.23	0.00

In summary, reduced precipitation and significant temperature increases restrained vegetation growth at elevations lower than 300m by limiting soil water.

4.3. Other Factors Affecting Vegetation in the High-Elevation Gradient

Snow cover changes are known to affect vegetation [35,70,71], but the SEM results show a small PC of snow cover on the NDVI (Figure 5). This could be because some intermediate variables (runoff, permafrost, soil water, etc.) between snow cover and vegetation are difficult to quantify in the model. As the highest elevation in ACA, some areas of Tianshan are covered by permanent glaciers and year-round snow, and many rivers originate from Tianshan [72]. Therefore, with global warming, the impact of changes in glaciers and snow cover on vegetation in the study area is not negligible. First, warming results in shrinking glaciers and snow cover, such as Urumqi Glacier No. 1 [29], leading to an increase in runoff [72]. For example, the runoff from the Urumqi River in eastern ACA has increased significantly since the 1980s [73]. The increase in runoff provides sufficient water for vegetation growth. At the same time, the presence of a highly relevant element to these elements, permafrost, also allows for the development of various vegetation types. In summary, warming-induced shrinkage of glaciers and a reduction in snow cover thus causes an increase in runoff and soil water which has a positive effect on vegetation greening.

The specific physical mechanisms and eco-hydrological processes involved still need investigation, even though this study examined the elements influencing vegetation change in ACA from simple to complicated factors. Furthermore, it is also essential to investigate how vegetation will evolve due to prolonged global warming.

5. Conclusions

This paper analyzes the antiphase trends of vegetation and meteorological variables in ACA. We quantified the direct and indirect factors affecting vegetation using NDVI data from remote sensing observation and reanalysis data of meteorological variables. The conclusions are as follows:

(1) Growing season NDVI in ACA experienced greening at a rate of 0.0002 yr^{-1} from 1982 to 2015. In addition, an antiphase trend was observed with a boundary at an elevation of 300 m. Specifically, the eastern part of ACA is greening (elevations higher than 300 m), while the western part of ACA is browning (elevations lower than 300 m).

(2) Based on the results of LMM, vegetation is mainly influenced by precipitation and soil water, and differences in elevation and vegetation types explain most residuals.

(3) The results of SEM show that soil water plays a leading role in vegetation dynamics at an elevation lower than 300 m, while the area higher than 300 m is mainly influenced by precipitation. The temperature has an indirect effect on vegetation by affecting precipitation and soil water.

(4) Growing season vegetation has a lagging response to winter precipitation in areas with an elevation lower than 300 m.

References

1. Li, Z.; Chen, Y.; Li, W.; Deng, H.; Fang, G. Potential impacts of climate change on vegetation dynamics in Central Asia. *J. Geophys Res. Atmos.* **2015**, *120*, 12345–12356. [CrossRef]
2. Zhao, Y.S. *Principles and Methods of Remote Sensing Application Analysis*; Science Press: Beijing, China, 2003; pp. 413–416.
3. Zhao, X.; Tan, K.; Zhao, S.; Fang, J. Changing climate affects vegetation growth in the arid region of the northwestern China. *J. Arid Environ.* **2011**, *75*, 946–952. [CrossRef]
4. Seddon, A.W.R.; Macias-Fauria, M.; Long, P.R.; Benz, D.; Willis, K.J. Sensitivity of global terrestrial ecosystems to climate variability. *Nature* **2016**, *531*, 229–232. [CrossRef]
5. Yuan, Y.; Bao, A.M.; Liu, T.; Zheng, G.X.; Jiang, L.L.; Guo, H.; Jiang, P.; Yu, T.; de Maeyer, P. Assessing vegetation stability to climate variability in Central Asia. *J. Environ. Manag.* **2021**, *298*, 113330. [CrossRef] [PubMed]
6. Yin, G.; Hu, Z.Y.; Chen, X.; Tiyip, T. Vegetation dynamics and its response to climate change in Central Asia. *J. Arid Land* **2016**, *8*, 375–388. [CrossRef]
7. Zhang, Y.; Gentine, P.; Luo, X.; Lian, X.; Liu, Y.; Zhou, S.; Michalak, A.M.; Sun, W.; Fisher, J.B.; Piao, S.; et al. Increasing sensitivity of dryland vegetation greenness to precipitation due to rising atmospheric CO2. *Nat. Commun.* **2022**, *13*, 4875. [CrossRef] [PubMed]
8. Jiang, L.L.; Guli, J.; Bao, A.M.; Guo, H.; Ndayisaba, F. Vegetation dynamics and responses to climate change and human activities in Central Asia. *Sci. Total Environ.* **2017**, *599–600*, 967–980. [CrossRef]
9. Wang, X.H.; Piao, S.L.; Ciais, P.; Li, J.S.; Friedlingstein, P.; Koven, C.; Chen, A.P. Spring temperature change and its implication in the change of vegetation growth in North America from 1982 to 2006. *Proc. Natl. Acad. Sci. USA* **2011**, *108*, 1240–1245. [CrossRef]
10. Liu, X.D.; Ma, Q.H.; Yu, H.Y.; Li, Y.B.; Li, L.; Qi, M.; Wu, W.J.; Zhang, F.; Wang, Y.H.; Zhou, G.S.; et al. Climate warming-induced drought constrains vegetation productivity by weakening the temporal stability of the plant community in an arid grassland ecosystem. *Agr. Forest Meteorol.* **2021**, *307*, 108526. [CrossRef]
11. Feng, X.M.; Fu, B.J.; Zhang, Y.; Pan, N.Q.; Zeng, Z.Z.; Tian, H.Q.; Lyu, Y.H.; Chen, Y.Z.; Ciais, P.; Wang, Y.P.; et al. Recent leveling off of vegetation greenness and primary production reveals the increasing soil water limitations on the greening Earth. *Sci. Bull.* **2021**, *66*, 1462–1471. [CrossRef]
12. Li, Y.P.; Chen, Y.N.; Sun, F.; Li, Z. Recent vegetation browning and its drivers on Tianshan Mountain, Central Asia. *Ecol. Indic.* **2021**, *129*, 107912. [CrossRef]
13. Zhang, W.; Li, Y.; Wu, X.C.; Chen, Y.H.; Chen, A.P.; Schwalm, C.R.; Kimball, J.S. Divergent Response of Vegetation Growth to Soil Water Availability in Dry and Wet Periods Over Central Asia. *J. Geophys. Res. Biogeosci.* **2021**, *126*, e2020JG005912. [CrossRef]
14. Yao, J.Q.; Hu, W.F.; Chen, Y.N.; Huo, W.; Zhao, Y.; Mao, W.Y.; Yang, Q. Hydro-climatic changes and their impacts on vegetation in Xinjiang, Central Asia. *Sci. Total Environ.* **2019**, *660*, 724–732. [CrossRef] [PubMed]
15. Peng, X.; Zhang, T.; Frauenfeld, O.W.; Wang, S.; Qiao, L.; Du, R.; Mu, C. Northern Hemisphere Greening in Association With Warming Permafrost. *J. Geophys. Res. Biogeosci.* **2020**, *125*, 2742. [CrossRef]
16. Wang, J.; Liu, D.S. Vegetation green-up date is more sensitive to permafrost degradation than climate change in spring across the northern permafrost region. *Glob. Chang. Biol.* **2022**, *28*, 1569–1582. [CrossRef] [PubMed]
17. Huang, W.; Chen, J.H.; Zhang, X.J.; Feng, S.; Chen, F.H. Definition of the core zone of the "westerlies-dominated climatic regime", and its controlling factors during the instrumental period. *Sci. China Earth Sci.* **2015**, *58*, 676–684. [CrossRef]
18. Lioubimtseva, E.; Henebry, G.M. Climate and environmental change in arid Central Asia: Impacts, vulnerability, and adaptations. *J. Arid Environ.* **2009**, *73*, 963–977. [CrossRef]
19. Huang, J.; Yu, H.; Guan, X.; Wang, G.; Guo, R. Accelerated dryland expansion under climate change. *Nat. Clim. Chang.* **2016**, *6*, 166–171. [CrossRef]
20. Huang, W.; Chang, S.Q.; Xie, C.L.; Zhang, Z.P. Moisture sources of extreme summer precipitation events in North Xinjiang and their relationship with atmospheric circulation. *Adv. Clim. Chang. Res.* **2017**, *8*, 12–17. [CrossRef]
21. Chen, F.H.; Huang, W. Multi-scale climate variations in the arid Central Asia. *Adv Clim Chang. Res.* **2017**, *8*, 1–2. [CrossRef]
22. Xie, T.T.; Huang, W.; Chang, S.Q.; Zheng, F.; Chen, J.H.; Chen, J.; Chen, F.H. Moisture sources of extreme precipitation events in arid Central Asia and their relationship with atmospheric circulation. *Int. J. Climatol.* **2021**, *41*, 497. [CrossRef]

23. Zhou, Y.; Zhang, L.; Fensholt, R.; Wang, K.; Vitkovskaya, I.; Tian, F. Climate Contributions to Vegetation Variations in Central Asian Drylands: Pre- and Post-USSR Collapse. *Remote Sens.* **2015**, *7*, 2449–2470. [CrossRef]
24. Hao, H.; Chen, Y.; Xu, J.; Li, Z.; Li, Y.; Kayumba, P.M. Water Deficit May Cause Vegetation Browning in Central Asia. *Remote Sens.* **2022**, *14*, 2574. [CrossRef]
25. Zhao, R.; Liu, X.; Dong, J.; Zhao, G.; Manevski, K.; Andersen, M.N.; Tang, Q. Human activities modulate greening patterns: A case study for southern Xinjiang in China based on long time series analysis. *Environ. Res. Lett.* **2022**, *17*, 44012. [CrossRef]
26. Zhou, Y.; Li, Y.; Li, W.; Li, F.; Xin, Q. Ecological Responses to Climate Change and Human Activities in the Arid and Semi-Arid Regions of Xinjiang in China. *Remote Sens.* **2022**, *14*, 3911. [CrossRef]
27. Gao, M.; Piao, S.; Chen, A.; Yang, H.; Liu, Q.; Fu, Y.H.; Janssens, I.A. Divergent changes in the elevational gradient of vegetation activities over the last 30 years. *Nat. Commun.* **2019**, *10*, 2970. [CrossRef]
28. Zhu, M.; Zhang, J.; Zhu, L. Article Title Variations in Growing Season NDVI and Its Sensitivity to Climate Change Responses to Green Development in Mountainous Areas. *Front. Environ. Sci.* **2021**, *9*, 8450. [CrossRef]
29. Shi, Y.F.; Shen, Y.P.; Kang, E.; Li, D.L.; Ding, Y.J.; Zhang, G.W.; Hu, R.J. Recent and Future Climate Change in Northwest China. *Climatic Chang.* **2007**, *80*, 379–393. [CrossRef]
30. Peng, D.D.; Zhou, T.J. Why was the arid and semiarid northwest China getting wetter in the recent decades? *J. Geophys. Res. Atmos.* **2017**, *122*, 9060–9075. [CrossRef]
31. Yao, J.Q.; Chen, Y.N.; Guan, X.F.; Zhao, Y.; Chen, J.; Mao, W.Y. Recent climate and hydrological changes in a mountain–basin system in Xinjiang, China. *Earth-Sci. Rev.* **2022**, *226*, 103957. [CrossRef]
32. Hu, Z.; Chen, X.; Chen, D.; Li, J.; Wang, S.; Zhou, Q.; Yin, G.; Guo, M. "Dry gets drier, wet gets wetter": A case study over the arid regions of central Asia. *Int. J. Climatol.* **2019**, *39*, 1072–1091. [CrossRef]
33. Feng, S.; Fu, Q. Expansion of global drylands under a warming climate. *Atmos. Chem. Phys.* **2013**, *13*, 10081–10094. [CrossRef]
34. Chen, F.; Wang, J.; Jin, L.; Zhang, Q.; Li, J.; Chen, J. Rapid warming in mid-latitude central Asia for the past 100 years. *Front. Earth Sci. China* **2009**, *3*, 42–50. [CrossRef]
35. Paudel, K.P.; Andersen, P. Response of rangeland vegetation to snow cover dynamics in Nepal Trans Himalaya. *Climatic Chang.* **2013**, *117*, 149–162. [CrossRef]
36. Geng, L.; Che, T.; Wang, X.; Wang, H. Detecting Spatiotemporal Changes in Vegetation with the BFAST Model in the Qilian Mountain Region during 2000–2017. *Remote Sens.* **2019**, *11*, 103. [CrossRef]
37. Tucker, C.J.; Pinzon, J.E.; Brown, M.E.; Slayback, D.A.; Pak, E.W.; Mahoney, R.; Vermote, E.F.; El Saleous, N. An extended AVHRR 8-km NDVI dataset compatible with MODIS and SPOT vegetation NDVI data. *Int. J. Remote Sens.* **2005**, *26*, 4485–4498. [CrossRef]
38. Holben, B.N. Characteristics of maximum-value composite images from temporal AVHRR data. *Int. J. Remote Sens.* **1986**, *7*, 1417–1434. [CrossRef]
39. Schneider, U.; Becker, A.; Finger, P.; Rustemeier, E.; Ziese, M. GPCC Full Data Monthly Product Version 2020 at 0.25: Monthly Land-Surface Precipitation from Rain-Gauges Built on GTS-Based and Historical Data. *Glob. Precip. Climatol. Cent. (GPCC) Dtsch. Wetterd.* **2020**, 1–13. [CrossRef]
40. Harris, I.; Osborn, T.J.; Jones, P.; Lister, D. Version 4 of the CRU TS monthly high-resolution gridded multivariate climate dataset. *Sci. Data.* **2020**, *7*, 109. [CrossRef]
41. Muñoz Sabater, J. ERA5-Land monthly averaged data from 1981 to present. Copernicus Climate Change Service (C3S). *Clim. Data Store (CDS)* **2019**, *146*, 1999–2049.
42. Deng, Y.H.; Wang, S.J.; Bai, X.Y.; Luo, G.J.; Wu, L.H.; Chen, F.; Wang, J.F.; Li, C.J.; Yang, Y.J.; Hu, Z.Y.; et al. Vegetation greening intensified soil drying in some semi-arid and arid areas of the world. *Agr. Forest Meteorol.* **2020**, *292–293*, 108103. [CrossRef]
43. Chen, C.; Park, T.; Wang, X.H.; Piao, S.L.; Xu, B.D.; Chaturvedi, R.K.; Fuchs, R.; Brovkin, V.; Ciais, P.; Fensholt, R.; et al. China and India lead in greening of the world through land-use management. *Nat. Sustain.* **2019**, *2*, 122–129. [CrossRef]
44. Zhu, Z.C.; Piao, S.L.; Myneni, R.B.; Huang, M.T.; Zeng, Z.Z.; Canadell, J.G.; Ciais, P.; Sitch, S.; Friedlingstein, P.; Arneth, A.; et al. Greening of the Earth and its drivers. *Nature Clim. Chang.* **2016**, *6*, 791–795. [CrossRef]
45. Piao, S.L.; Wang, X.H.; Park, T.; Chen, C.; Lian, X.; He, Y.; Bjerke, J.W.; Chen, A.P.; Ciais, P.; Tømmervik, H.; et al. Characteristics, drivers and feedbacks of global greening. *Nat. Rev. Earth Environ.* **2020**, *1*, 14–27. [CrossRef]
46. Brown, D.; Brownrigg, R.; Haley, M.; Huang, W. *NCAR Command Language (NCL)*; UCAR/NCAR-Computational and Information Systems Laboratory (CISL), 2012. Available online: https://www.ncl.ucar.edu/ (accessed on 13 October 2022).
47. Du, J.; He, Z.B.; Piatek, K.B.; Chen, L.F.; Lin, P.F.; Zhu, X. Interacting effects of temperature and precipitation on climatic sensitivity of spring vegetation green-up in arid mountains of China. *Agr. Forest Meteorol.* **2019**, *269–270*, 71–77. [CrossRef]
48. Zuidema, P.A.; Heinrich, I.; Rahman, M.; Vlam, M.; Zwartsenberg, S.A.; van der Sleen, P. Recent CO_2 rise has modified the sensitivity of tropical tree growth to rainfall and temperature. *Glob. Chang. Biol.* **2020**, *26*, 4028–4041. [CrossRef] [PubMed]
49. Schnabel, F.; Liu, X.J.; Kunz, M.; Barry, K.E.; Bongers, F.J.; Bruelheide, H.; Fichtner, A.; Härdtle, W.; Li, S.; Pfaff, C.-T.; et al. Species richness stabilizes productivity via asynchrony and drought-tolerance diversity in a large-scale tree biodiversity experiment. *Sci. Adv.* **2021**, *7*, eabk1643. [CrossRef]
50. Reich, P.B.; Sendall, K.M.; Stefanski, A.; Rich, R.L.; Hobbie, S.E.; Montgomery, R.A. Effects of climate warming on photosynthesis in boreal tree species depend on soil moisture. *Nature* **2018**, *562*, 263–267. [CrossRef]
51. R Core Team. *R: A Language and Environment for Statistical Computing*; R Foundation for Statistical Computing: Vienna, Austria, 2016. Available online: http://www.R-project.org (accessed on 17 November 2022).

52. Bates, D. lme4: Linear Mixed-Effects Models Using S4 Classes. R Package Version 0.999375-33. 2010. Available online: https://cran.r-project.org/web/packages/lme4/index.html (accessed on 17 November 2022).

53. Kuznetsova, A.; Brockhoff, P.B.; Christensen, R.H.B. lmerTest package: Tests in linear mixed effects models. *J. Stat. Softw.* **2017**, *82*, 1–26. [CrossRef]

54. Lin, L.C.; Huang, P.H.; Weng, L.J. Selecting Path Models in SEM: A Comparison of Model Selection Criteria. Structural Equation Modeling. *A Multidiscip. J.* **2017**, *24*, 855–869. [CrossRef]

55. Kline, R.B. Software review: Software programs for structural equation modeling: Amos, EQS, and LISREL. *J. Psychoeduc. Assess.* **1998**, *16*, 343–364. [CrossRef]

56. Arbuckle, J.L. *Amos*, Version 24.0; Computer Program; IBM SPSS: Chicago, IL, USA, 2019.

57. Rosseel, Y. lavaan: An R Package for Structural Equation Modeling. *J. Stat. Soft.* **2012**, 48. [CrossRef]

58. Xue, J.; Wang, Y.Y.; Teng, H.F.; Wang, N.; Li, D.L.; Peng, J.; Biswas, A.; Shi, Z. Dynamics of Vegetation Greenness and Its Response to Climate Change in Xinjiang over the Past Two Decades. *Remote Sens.* **2021**, *13*, 4063. [CrossRef]

59. Zheng, K.; Tan, L.; Sun, Y.; Wu, Y.; Duan, Z.; Xu, Y.; Gao, C. Impacts of climate change and anthropogenic activities on vegetation change: Evidence from typical areas in China. *Ecol. Indic.* **2021**, *126*, 107648. [CrossRef]

60. Holdridge, L.R. Determination of World Plant Formations from Simple Climatic Data. *Science* **1947**, *105*, 367–368. [CrossRef] [PubMed]

61. Whittaker, R.H. Classification of natural communities. *Bot. Rev* **1962**, *28*, 1–239. [CrossRef]

62. Walter, H.; Box, E. Global classification of natural terrestrial ecosystems. *Plant Ecol.* **1976**, *32*, 75–81. [CrossRef]

63. Chen, F.; Huang, W.; Jin, L.; Chen, J.; Wang, J. Spatiotemporal precipitation variations in the arid Central Asia in the context of global warming. *Sci. China Earth Sci.* **2011**, *54*, 1812–1821. [CrossRef]

64. Wu, D.H.; Zhao, X.; Liang, S.L.; Zhou, T.; Huang, K.C.; Tang, B.J.; Zhao, W.Q. Time-lag effects of global vegetation responses to climate change. *Glob. Chang. Biol.* **2015**, *21*, 3520–3531. [CrossRef]

65. Burrell, A.L.; Evans, J.P.; de Kauwe, M.G. Anthropogenic climate change has driven over 5 million km2 of drylands towards desertification. *Nat. Commun.* **2020**, *11*, 3853. [CrossRef]

66. Maestre, F.T.; Benito, B.M.; Berdugo, M.; Concostrina-Zubiri, L.; Delgado-Baquerizo, M.; Eldridge, D.J.; Guirado, E.; Gross, N.; Kéfi, S.; Le Bagousse-Pinguet, Y.; et al. Biogeography of global drylands. *New Phytol.* **2021**, *231*, 540–558. [CrossRef] [PubMed]

67. Hickler, T.; Eklundh, L.; Seaquist, J.W.; Smith, B.; Ardö, J.; Olsson, L.; Sykes, M.T.; Sjöström, M. Precipitation controls Sahel greening trend. *Geophys. Res. Lett.* **2005**, *32*, 193. [CrossRef]

68. Mo, K.; Chen, Q.W.; Chen, C.; Zhang, J.Y.; Wang, L.; Bao, Z.X. Spatiotemporal variation of correlation between vegetation cover and precipitation in an arid mountain-oasis river basin in northwest China. *J. Hydrol.* **2019**, *574*, 138–147. [CrossRef]

69. Moore, G.W.; Jones, J.A.; Bond, B.J. How soil moisture mediates the influence of transpiration on streamflow at hourly to interannual scales in a forested catchment. *Hydrol. Process.* **2011**, *25*, 3701–3710. [CrossRef]

70. Dye, D.G.; Tucker, C.J. Seasonality and trends of snow-cover, vegetation index, and temperature in northern Eurasia. *Geophys. Res. Lett.* **2003**, 30. [CrossRef]

71. Johansson, M.; Callaghan, T.V.; Bosiö, J.; Åkerman, H.J.; Jackowicz-Korczynski, M.; Christensen, T.R. Rapid responses of permafrost and vegetation to experimentally increased snow cover in sub-arctic Sweden. *Environ. Res. Lett.* **2013**, *8*, 35025. [CrossRef]

72. Sorg, A.; Bolch, T.; Stoffel, M.; Solomina, O.; Beniston, M. Climate change impacts on glaciers and runoff in Tien Shan (Central Asia). *Nat. Clim. Chang.* **2012**, *2*, 725–731. [CrossRef]

73. Li, Z.Q.; Wang, W.B.; Zhang, M.J.; Wang, F.T.; Li, H.L. Observed changes in streamflow at the headwaters of the Urumqi River, eastern Tianshan, central Asia. *Hydrol. Process.* **2009**, *24*, 217–224. [CrossRef]